



## IN-FLOW CALIBRATION APPROACH FOR IMPROVING BEAMFORMING ACCURACY

S. Kroeber and K. Ehrenfried and L. Koop and A. Lauterbach  
German Aerospace Center (DLR)  
Bunsenstrasse 10, 37073 Goettingen, Germany  
email: stefan.kroeber@dlr.de

The phased microphone array technique is a well established tool in aeroacoustic testing for the localisation and quantification of sound sources. The measurements are often carried out in closed or open wind tunnels using scaled models. In both types of wind tunnels flow effects derogate the accuracy of beamforming results. In the open test-section the sound waves have to pass through the wind tunnel shear layer before reaching the microphone. That results in a spatial coherence loss due to turbulent scattering and refraction and potentially leads to degraded source maps and under-estimated source levels. The present study addresses this matter and proposes a calibration approach for an open wind tunnel using an in-flow calibration source. This source employs a ribbon loudspeaker which can provide sufficiently high sound pressure levels in a broad frequency range and its properties are known. The presented results comprise details of the applied in-flow calibration sound source, the calibration procedure and its evaluation with respect to the achieved beamforming accuracy.

### 1 INTRODUCTION

Aeroacoustic testing is often carried out in open jet wind tunnels. Typically, the model is placed inside the potential core of the jet and the microphones locations are outside the flow. Hence, the sound waves emitted from aeroacoustic sources of the model have to pass through the wind tunnel shear layer before reaching the microphone. This sound propagation through a turbulent shear layer is accompanied by several effects which may influence the beamforming accuracy. Fig. 1 illustrates this particular situation. The source, located in the potential core of the jet, emits a wave and the convection of the wave takes place due to the parallel flow until the turbulent shear layer is reached. While propagating through the shear layer the incoming sound waves are refracted. When the shear layer has a curvature the sound refraction can result in the

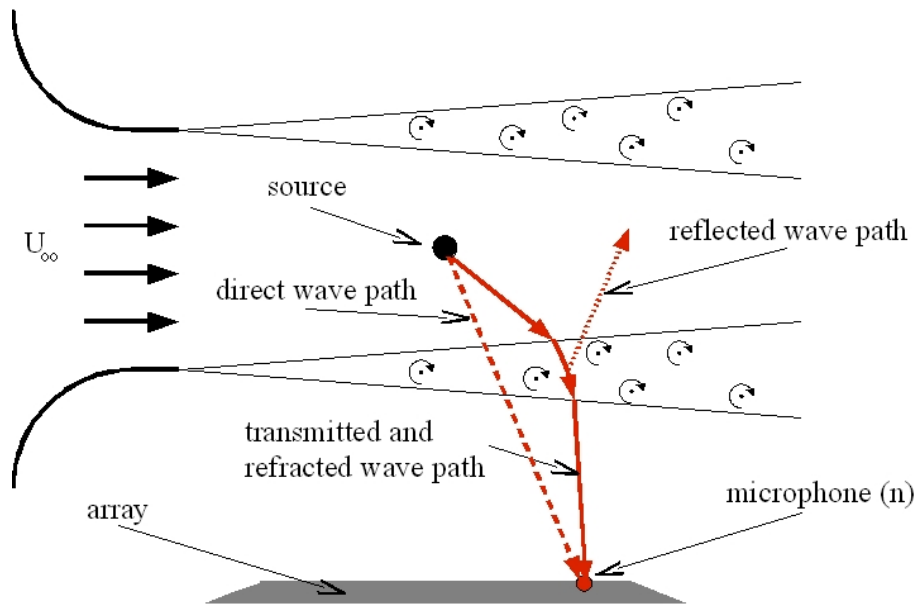


Figure 1: Schematic sketch for microphone array measurements in open jet wind tunnels

formation of a caustic where interferences can occur (Pierce [9]). In addition, only a part of the incident acoustic wave energy is transmitted to the microphone while the rest is reflected. On the one hand under certain conditions which depend on the open jet Mach-number and the geometrical setup, total reflection is possible and no transmission of acoustic energy takes place in distinct areas and therefore no sound can be measured outside the flow. On the other hand multiple reflections can occur and the sound from a source can reach the observer along different paths. In this case the observer will be unable to distinguish the two contributions without some additional information. Furthermore, the sound waves are scattered at turbulent structures in the shear layer. This leads to a reallocation of acoustic energy of the sound wave into other propagation directions and frequencies. All mentioned effects lead to variations in the travel time of the sound wave from the source to the observer. This is equivalent to a phase shift between source and microphone when the analysis is carried out in the frequency domain. If these phase variations are not taken into account in the beamforming process it will result in a performance loss of the source maps. In order to address this matter, many analytical and numerical methods have been developed and subsequently published by various authors. Many concepts are based on a simplified flow model, for example a plane or round shear layer with constant or zero thickness, as presented by Amiet [2], Ahuja et al. [1], Morfey [7]. The computational effort is normally easy to manage, but the validity is limited. The method of Candel [3] solves numerically the ray equations so that an arbitrary three-dimensional flow can be treated. Such an approach requires that the flow-field is known and the determination of the flow-field can be very extensive. A totally numerical method has been proposed by Kornow [5]. The flow-field of the open jet wind tunnel is firstly calculated by a numerical simulation and then, in a second step, an acoustic source is placed within the flow and the sound propagation through the flow is computed numerically. The final numerical results can be used to correct the phase variations.

In the present paper an experimental in-flow calibration procedure using a novel in-flow calibration sound source is proposed to correct for these phase variations in open jet wind tunnels in order to improve the beamforming accuracy. This approach has the advantage that no information about the flow-field is required. All kinds of shear layer geometries and flow-fields can be calibrated with this method. The shown results comprise details of the applied in-flow calibration sound source, the calibration procedure and its evaluation with respect to the achieved beamforming accuracy. Finally, the obtained calibration results are compared with the flow correction results for the plane, zero thickness shear layer model of Amiet [2].

## 2 OUTLINE OF THE IN-FLOW CALIBRATION APPROACH

### 2.1 Delay and sum beamformer

The frequency-dependent output  $A(\omega, \mathbf{x}_s)$  of the delay and sum beamformer (DSB) for the source power of a monopole source at a scan point  $\mathbf{x}_s$  can be written as:

$$A(\omega, \mathbf{x}_s) = \frac{\mathbf{w}^H(\omega, \mathbf{x}_s) \mathbf{R}(\omega, \mathbf{x}_s) \mathbf{w}(\omega, \mathbf{x}_s)}{m^2}, \quad (1)$$

whereas  $\mathbf{R}$  is the cross correlation matrix,  $m$  the number of microphones and  $(\cdot)^H$  denotes the conjugate complex transposed vector. The variable

$$\mathbf{w}(\omega, \mathbf{x}_s) = \begin{pmatrix} \frac{e^{-i\Delta\varphi_1}}{|\mathbf{x}_1 - \mathbf{x}_s|} \\ \frac{e^{-i\Delta\varphi_2}}{|\mathbf{x}_2 - \mathbf{x}_s|} \\ \vdots \\ \frac{e^{-i\Delta\varphi_m}}{|\mathbf{x}_m - \mathbf{x}_s|} \end{pmatrix} \quad (2)$$

represents the steering vector with amplitude correction for a monopole source. It is essential to know the exact phase shift of the sound wave from the source location  $\mathbf{x}_s$  to all microphone positions  $\mathbf{x}_n$  for the beamforming process. Without flow the signal phase shift can easily be computed by

$$\Delta\varphi_n = \frac{\omega |\mathbf{x}_n - \mathbf{x}_s|}{c}, \quad (3)$$

provided that the speed of sound  $c$ , the microphone and source positions are known. In the case with flow the situation is much more complicated and several effects, as discussed in the introduction in section 1, have an influence on the wave travel path and subsequently, also on the phase shift, too. The following modification of eq.(3) takes this fact into account:

$$\Delta\varphi_{n,mod} = \Delta\varphi_n + \Delta\varphi_{n,flow}. \quad (4)$$

The additional parameter  $\Delta\varphi_{n,flow}$  represents all phase shifts caused by the flow.

## 2.2 Calibration procedure

The following describes how  $\Delta\varphi_{n,flow}$  can be experimentally determined using an in-flow calibration sound source. The calibration source is placed at the position where the model is to be installed. The source generates a broadband sound field which should coincide with the measured frequency band of the aeroacoustic sources of the examined model. Now, one performs a microphone array measurement without flow and computes sources maps using the DSB. For each analysis frequency the source maximum position in the map  $\mathbf{x}_{s,max}(\omega)$  is determined. Performing this procedure again, but this time with flow, the source maximum  $\mathbf{x}_{s,max,flow}(\omega)$  will be shifted due to the influence of the flow on the sound wave propagation. This source maximum displacement in the maps can be used to define a frequency-dependent diagonal calibration matrix

$$\mathbf{C}_{cal}(\omega) = \begin{pmatrix} C_1 & 0 & \dots & 0 \\ 0 & C_2 & \dots & 0 \\ \vdots & \vdots & \ddots & \vdots \\ 0 & 0 & \dots & C_m \end{pmatrix} \quad (5)$$

with the diagonal elements

$$C_n(\omega) = \frac{e^{i\frac{\omega|\mathbf{x}_n - \mathbf{x}_{s,max,flow}|}{c}}}{e^{i\frac{\omega|\mathbf{x}_n - \mathbf{x}_{s,max}|}{c}}}. \quad (6)$$

Finally, the calibrated cross correlation matrix results in

$$\mathbf{R}_{cal}(\omega) = \mathbf{C}_{cal}^H(\omega)\mathbf{R}(\omega)\mathbf{C}_{cal}(\omega). \quad (7)$$

A similar calibration procedure without flow was described by Mueller [8].

## 3 EXPERIMENT SETUP

### 3.1 The Aeroacoustic Wind Tunnel Braunschweig

The current investigation was conducted in the DLR Aeroacoustic Wind Tunnel Braunschweig (AWB) which is an open jet acoustic test facility. The nozzle has a rectangular exit with the dimensions 1.2 m  $\times$  0.8 m and a maximum flow velocity of 60 m/s. The measurements were carried out using an array of 144 microphones, arranged in nine logarithmic spiral arms with an aperture of 1 m. The fairing of the microphone array is made from aluminum and has a thickness of 25 mm. The array has already been used by Koop [4] for aeroacoustic measurements in closed wind tunnels. Fig. 2 shows the installation of both models in the wind tunnel with the microphone array on the right side, outside the flow. The data acquisition system VIPER-48 from GBM is located outside the test section. The microphone signals were simultaneously sampled with an AD conversion of 16-bit at a sampling frequency of  $f_s = 140$  kHz for all performed measurements. All channels had an antialiasing filter at  $f_u = 70$  kHz. The recording time for one measurement was 30 s. Band-pass filtered white noise, in the range of 7 kHz to 70 kHz, served as the loudspeaker input signal.

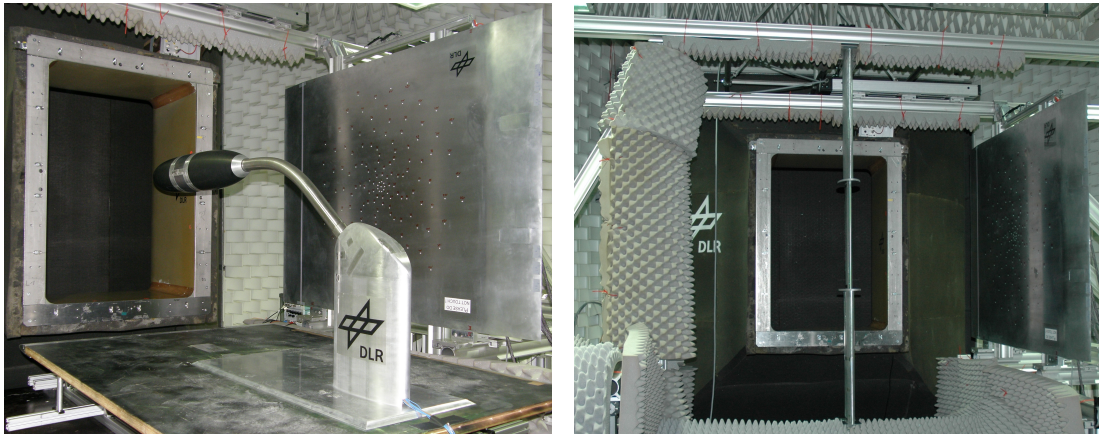


Figure 2: Installation of both models in the wind tunnel with the microphone array on the right side

### 3.2 IN-FLOW CALIBRATION SOUND SOURCE

The in-flow calibration source, shown in Fig. 3, was designed for all kinds of calibration issues in open and closed wind tunnels. The source employs a ribbon loudspeaker which can emit sufficiently high sound pressure levels in a broad frequency range up to 70 kHz. For in-flow applications the entire source is enclosed with symmetrical aerodynamic fairings. The ribbon diameter measures 90 mm and has a height of 15 mm. The loudspeaker membrane is recessed in a cavity in order to avoid direct flow-membrane interactions. In wind tunnel applications the flow passes over the cavity, at whose edge flow separation can occur, leading to broadband pressure instabilities. These can induce cavity resonances. A metal grid covered with silk, masking the cavity, reduces the instability excitation. Five flush-mounted microphones within the cavity can measure the near-field sound pressure fluctuations generated by the source. Sound generation of this type provides great flexibility in the spectral signal structure. Furthermore, it should be mentioned that the source is able to generate a partially monopole sound field. More details about the calibration source and its characteristics have been published in Kroeber et al [6].

### 3.3 PLATE WITH CAVITIES

The source used for the evaluation of the in-flow calibration approach incorporates an elliptically shaped plate with five different cavities, arranged in a line at various  $y$ -positions and consequently constitutes an aeroacoustic sound source with known positions. The cavities differ in shape and size to give sound emission in different frequency bands. Fig. 4 shows a sketch of the source. The plate is positioned between two end plates, after which follow elliptically shaped mountings. When the model is mounted in the open test section the plate with the cavities is located in the potential core of the jet with the flow velocity  $U_\infty$ . The elliptically shaped mountings are partially located in the potential core, partially in the turbulent shear layer and partially outside the flow. The end plates restrict the influence of the turbulent shear layer on the flow over the cavities.

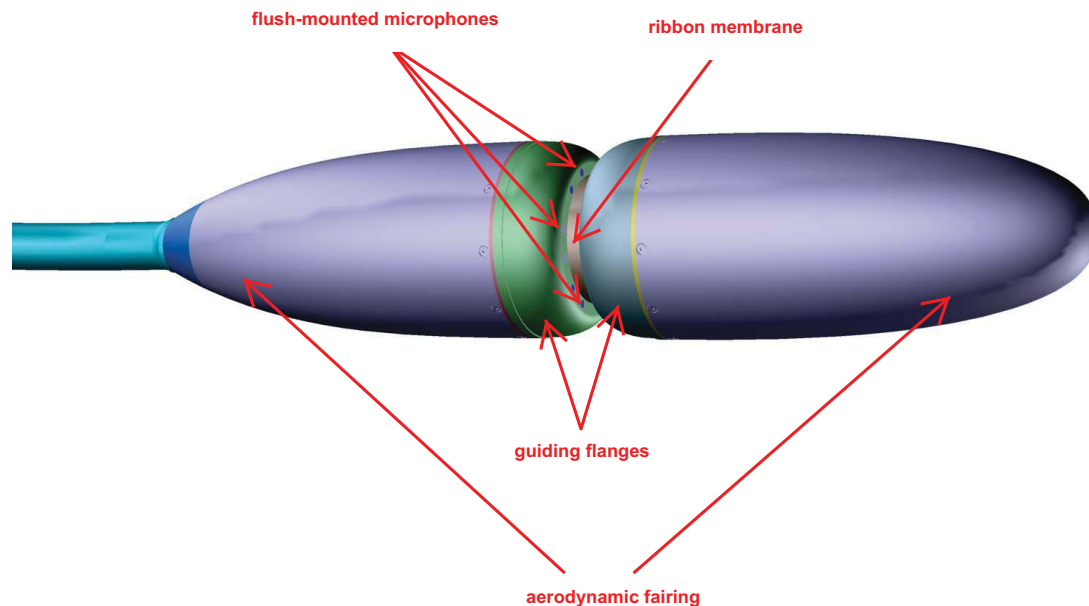


Figure 3: Sketch of the in-flow calibration sound source

### 3.4 Measurement procedure

In the first part of the examination the capabilities for aeroacoustic wind tunnel testing of the inflow-calibration source are evaluated. The second part contains the application and verification of the proposed in-flow calibration approach. The described procedure in section 2.2 is performed for various flow velocities. The membrane center of the calibration source was positioned at the latter location of cavity 2 ( $y = 0.1$  m) and the obtained calibration matrices  $\mathbf{C}_{cal}(\omega)$  are used to improve the beamforming results of the plate with cavities. The results for the maximum measured flow velocity  $U_\infty$  are shown in the next section.

## 4 EXPERIMENTAL RESULTS

### 4.1 Evaluation of the in-flow calibration sound source with flow

Fig. 5 shows typical 1/3 octave source maps of the calibration source for various flow velocities, computed with the DSB without flow corrections. The flow goes from left to right in the maps. At low frequencies, as shown by way of example for the case of 8 kHz, the source position is shifted downstream with increasing flow velocity in the maps as a result of the sound

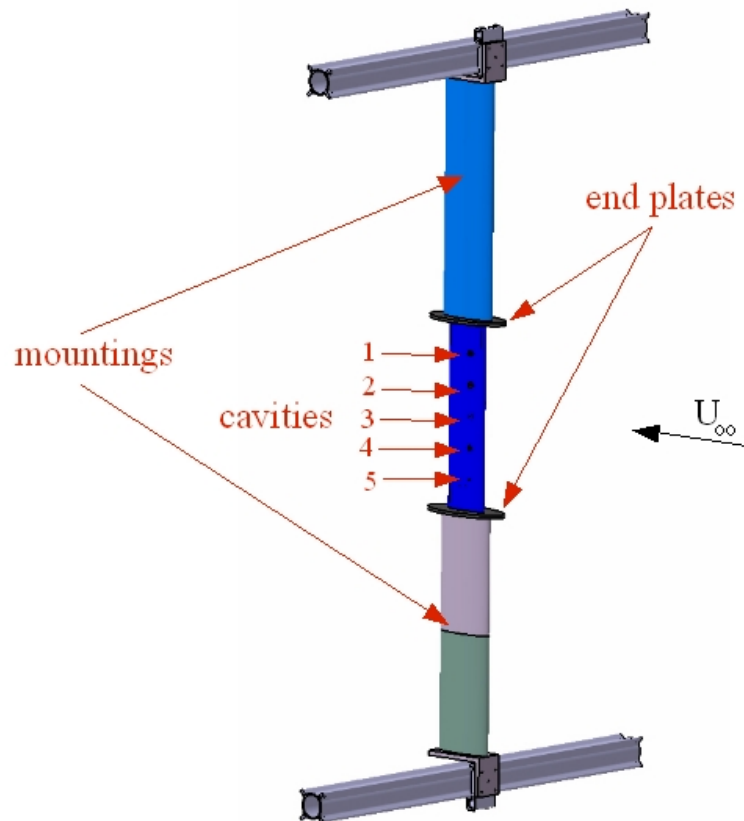


Figure 4: Sketch of the plate with cavities

propagation through the potential core and the shear layer of the jet. The calculated source power remains almost unaffected for all measured flow velocities and the signal-to-noise ratio in the maps does not change within the plotted range. A consideration of the 63 kHz case shows that turbulent scattering is much more dominant than at the lower frequency. The coherence loss caused by the turbulent shear layer degrades the signal-to-noise ratio significantly and the source area becomes bigger with increasing flow velocity. At  $U_\infty = 50 \text{ m/s}$  the source can no longer be identified.

#### 4.2 Results from the in-flow calibration approach

Fig. 6 shows beamforming results for selected 1/3 octave bands for  $U_\infty = 50 \text{ m/s}$  (flow coming from left to right, again) without flow correction, with in-flow calibration and with the Amiet

correction. The black box marks the position of the plate and the black circles the location of the cavities. Due to their various shapes and dimensions the cavities give birth to sound emissions in different frequency bands. Cavity 1 is a strong aeroacoustic source in the range of 4 kHz to 25 kHz and can easily be located with beamforming. The other cavities radiate sound at higher frequencies and can also be located accurately. An exception is cavity 3, where no source localization is possible, probably caused by a too low source strength. However, the plate can be used for the evaluation of the in-flow approach. Without flow correction the localized source positions differ from the original cavity locations. The in-flow calibration procedure corrects the source displacement over the entire frequency range and the localized sources match very well with the cavity positions. It is noteworthy that in this case the calibration matrices can be applied to a large area, although the calibration was performed for one point only. For example, cavity 5 is 0.3 m away from the position of the in-flow source during calibration, but one still obtains an excellent source localization result. This means that the part of the shear layer between the sources and the microphones does not dramatically change its characteristics with respect to sound refraction and transmission. The flow model of Amiet for the plane, zero thickness shear layer is a valid simplification for the current test setup, as verified by the beamforming results. The localized sources correspond to the cavity positions. Both methods, the in-flow calibration and the Amiet correction, yield results without significant differences.

## 5 CONCLUSIONS

The sound propagation through shear layers can decrease the microphone array performance in the beamforming process. Addressing this matter, a calibration approach using an in-flow calibration sound source was proposed and evaluated in an open jet acoustic wind tunnel. In the conducted test cases this procedure yielded excellent results, preparing path for further examinations. The performance of the approach using a more complicated model, for example a wing with high-lift system, should be investigated. Further tests should comprise the calibration possibilities of curved shear layers where the beamforming results using simplified flow models, such as the Amiet method, are often questionable.

## References

- [1] K.K. Ahuja, H.K. Tanna, and B.J. Tester. An experimental study of transmission, reflection and scattering of sound in a free jet flight simulation facility and comparison with theory. *Journal of Sound and Vibration*, 75(1):51–85, 1981.
- [2] R. K. Amiet. Refraction of sound by a shear layer. *Journal of Sound and Vibration*, 58(4): 467–482, 1978.
- [3] S.M Candel. Numerical solution of conservation equations arising in linear wave theory: Application to aeroacoustics. *Journal of Fluid Mechanics*, 83:465–493, 1977.
- [4] L. Koop. Microphone-array processing for wind-tunnel measurements with strong background noise. In *14th AIAA/CEAS Aeroacoustics Conference*, AIAA-Paper 2008-2907, Vancouver, Canada, 2008.

- [5] O. Kornow. Caa simulations of refraction of sound waves on a planar wind tunnel test section with its experimental verification. In *X3-Noise Scientific Workshop Bucharest, 2009*.
- [6] S. Kroeber, K. Ehrenfried, and L. Koop. Design and testing of sound sources for phased microphone array calibration. In *Second Berlin Beamforming Conference (BeBeC)*, Berlin, Germany, 2008.
- [7] C.L. Morfey and P.F. Joseph. Shear layer refraction corrections for off-axis sources in a jet flow. *Journal of Sound and Vibration*, 239(4):819–848, 2001.
- [8] T.J. Mueller. *Aeroacoustic Measurements*. Springer Verlag, 1. Auflage, 2002.
- [9] A. D. Pierce. *Acoustics: An Introduction to its Physical Principles and Applications*. McGraw-Hill, 1981.

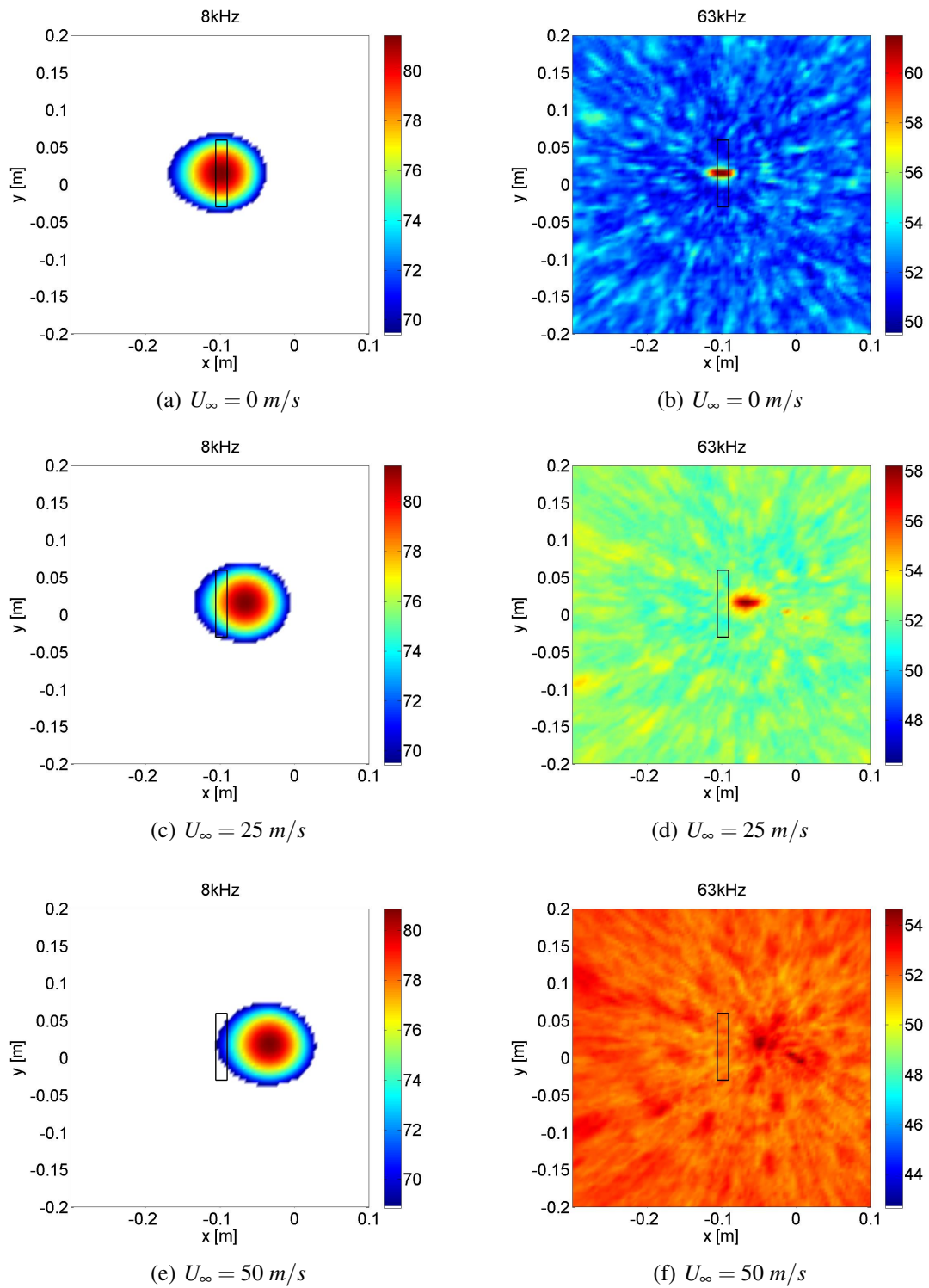


Figure 5: Beamforming results (in dB) without flow corrections of the in-flow calibration sound source for selected 1/3 octave bands for various flow velocities. The black box marks the position of the loudspeaker membrane.

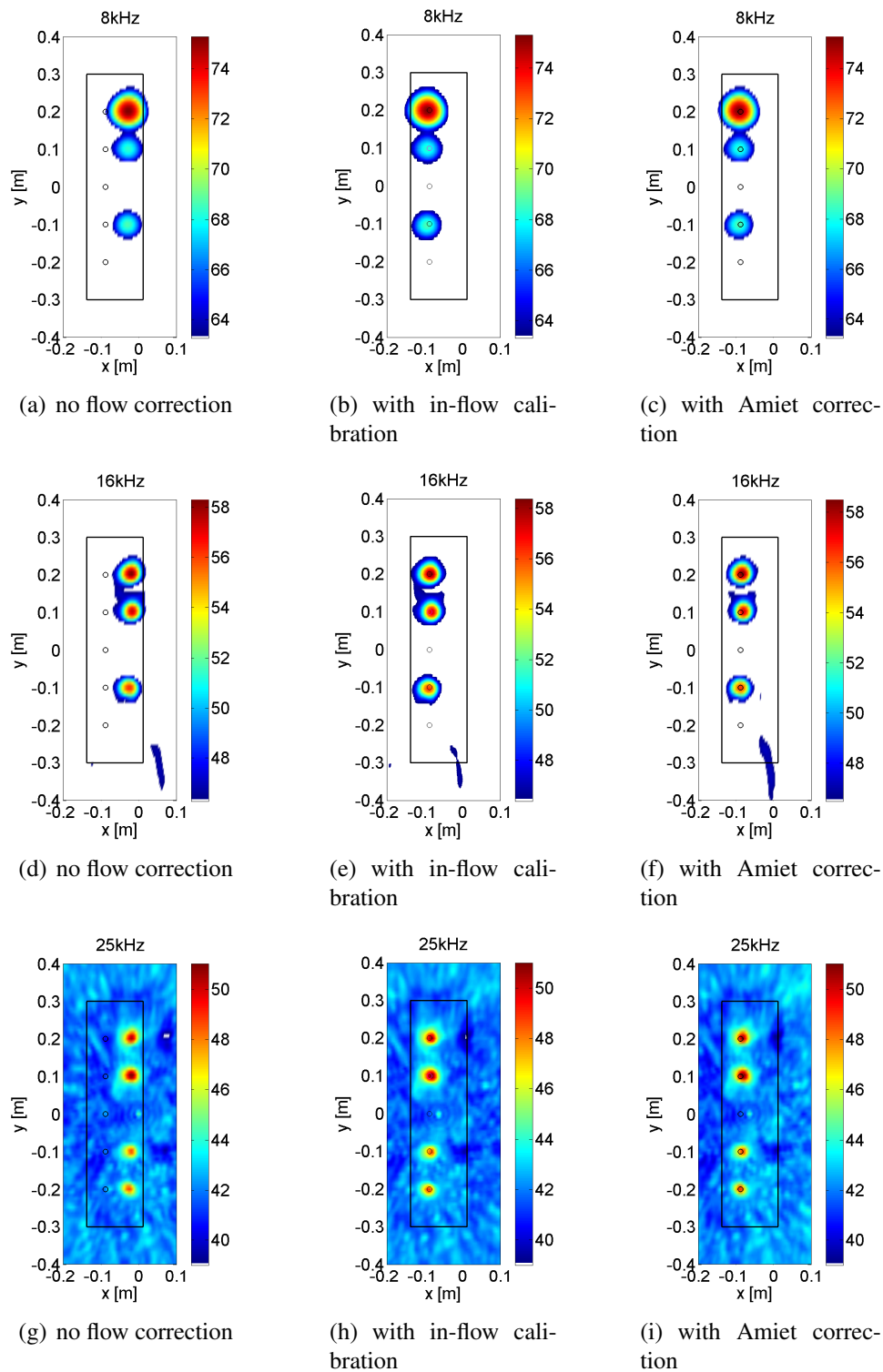


Figure 6: Beamforming results (in dB) of the plate with cavities for selected 1/3 octave bands for  $U_\infty = 50$  m/s without flow correction, with in-flow calibration and Amiet correction. The black box marks the position of the plate and the black circles the location of the cavities.